Earth and Planetary Science Letters 515 (2019) 221–230

Contents lists available at ScienceDirect

Earth and Planetary Science Letters

www.elsevier.com/locate/epsl

Low water content in the mantle source of the Hainan plume as a factor inhibiting the formation of a large igneous province

Xiao-Yan Gu [a,*], Piao-Yi Wang [b], Takeshi Kuritani [c], Eero Hanski [d], Qun-Ke Xia [a,*], Qin-Yan Wang [a]

[a] School of Earth Sciences, Zhejiang University, Hangzhou 310027, China
[b] School of Earth and Space Sciences, University of Science and Technology of China, Hefei 230026, China
[c] Graduate School of Science, Hokkaido University, 060-0810, Japan
[d] Oulu Mining School, University of Oulu, P.O. Box 3000, 90014 Oulu, Finland

ARTICLE INFO

Article history:
Received 12 December 2018
Received in revised form 22 March 2019
Accepted 24 March 2019
Available online 3 April 2019
Editor: T.A. Mather

Keywords:
large igneous provinces
water content
the southeastern Asian basalt province
the Hainan plume
Hainan basalts
clinopyroxene phenocrysts

ABSTRACT

Large igneous provinces (LIPs) are generally considered to be related to mantle plumes and to have a great importance to the supercontinent break-up events, climate change and biological evolution over Earth's history. The high melt production rates of LIPs can be achieved under rigorous melting conditions: an abnormally high temperature, substantial decompression, addition of fusible components, or remarkable enrichment in water. Although it has been repeatedly noticed that water enrichment has occurred in many Phanerozoic LIPs, the significance of water enrichment in the mantle source for the generation of LIPs has not been explicitly highlighted. The southeastern Asian basalt province (SABP), which is thought to have formed by the Hainan mantle plume from a pyroxenite-bearing source, was emplaced over a small area of about 0.037 Mkm^2 over a long period of time from 28.5 Ma to Holocene, thus differing from a typical LIP (>0.1 Mkm^3 in volume emplaced in one or multiple pulses of less than 5 Ma). In this work, we measured H_2O contents of high-Mg# clinopyroxene phenocrysts (12–179 ppm H_2O) from Cenozoic basalts in the northern Hainan Island, which is part of the SABP. These data were utilized to estimate the water content of the mantle source of these basalts, yielding values in the range of 84–360 ppm H_2O, which are significantly lower than those obtained for many Phanerozoic LIPs (thousands of ppm). After calculating the mantle potential temperature for the Hainan basalts about 170 °C higher than that for the MORB source mantle, we consider that the paucity of source water likely depressed the melt productivity and the velocity of plume upwelling, and induced the Hainan plume to stall at depths of 350–500 km, inhibiting the formation of a LIP by the Hainan plume, despite the occurrence of other favorable conditions. Hence, our results from the SABP provide evidence for the significance of water enrichment in the mantle source in the formation of LIPs. The low water content in the Hainan plume can be attributed to the incorporation of subducted slabs that had experienced significant dehydration.

1. Introduction

Large igneous provinces (LIPs) are generated by emplacement of a huge amount of mafic magmas (>0.1 Mkm^3 in volume) in one or multiple igneous pulses of short duration (generally 1–5 Ma) (Ernst et al., 2005; Bryan and Ernst, 2008). Such high magma production rates result from synergistic effects of a specific set of melting conditions, including an abnormally high temperature, substantial decompression, addition of fusible components (e.g., pyroxenites), and remarkable enrichment in volatiles (especially water) (Campbell, 2001). Among the diverse models put forward in previous studies (e.g., Richards et al., 1989; Campbell and Griffiths, 1990; Jones et al., 2002; Hales et al., 2005; Hole, 2015), mantle plumes have most widely been accepted as an explanation for the generation of LIPs. The role of water in the generation of LIPs has been strengthened recently (Cabato et al., 2015; Xia Q.K. et al., 2016; Liu et al., 2017; Ivanov et al., 2018). In the study of Liu et al. (2017), the water contents in the primary magmas of the Dali picrites in the Emeishan LIP were estimated to be 3.44 ± 0.89 wt.%, corresponding to a water content of >6000 ppm in the mantle source. Combining these results with the estimated amount of pyroxenite in the mantle source (~40–50 wt.%) and the calculated

* Corresponding authors.
E-mail addresses: gxy0823@zju.edu.cn (X.-Y. Gu), qkxia@zju.edu.cn (Q.-K. Xia).

https://doi.org/10.1016/j.epsl.2019.03.034
0012-821X/

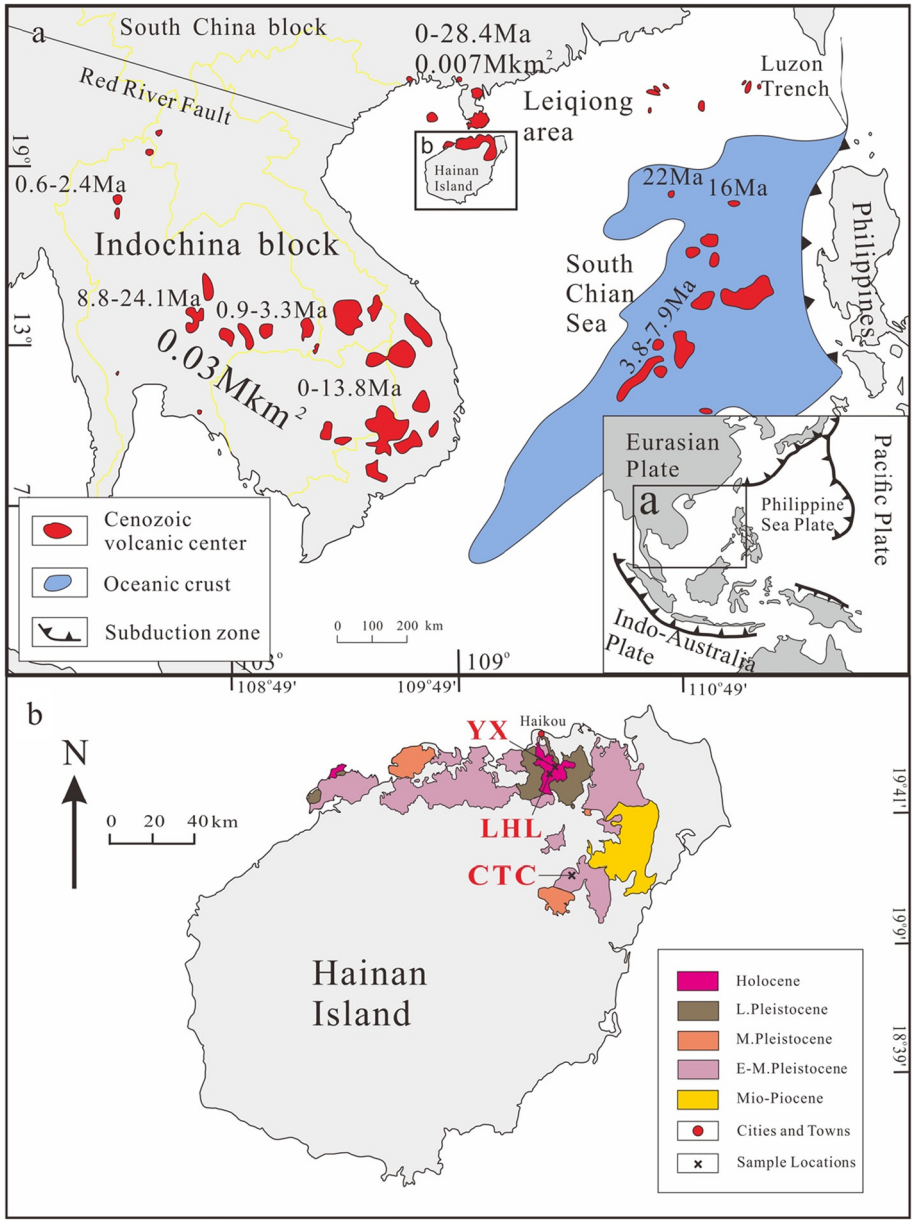

Fig. 1. (a) Distribution of Cenozoic basalts in southern Asia. The small sketch map is for the tectonic situation of the southern Asian basalt province (SABP). This area lies at the triple junction of the Eurasian, Indo-Australian and Pacific (Philippine) plates and is surrounded by multiple subduction zones. The SABP consists of continental Cenozoic basalts spreading over the Leiqiong area and the Indochina block. The Leiqiong area refers to the Leizhou Peninsula and the northern part of the Hainan Island. The whole SABP area is less than 0.037 Mkm^2 in extent. The map is modified from Yan et al. (2018). The ages and areas of individual basalts are from Yan et al. (2018), Hoang et al. (1996), and Ho et al. (2000). (b) Sampling locations of Cenozoic Hainan basalts in this study. The map is modified from Liu J.Q. et al. (2015).

olivine liquidus temperature (1460 ± 43 °C) for these picrites, it was proposed that a hydrous mantle plume rich in recycled components generated the Emeishan LIP. Based on data from several Phanerozoic continental LIPs, Liu et al. (2017) concluded that all the four factors (abnormally high temperature, substantial decompression, contribution of pyroxenite, and water enrichment) were involved in many continental LIPs (e.g., Emeishan LIP, Tarim LIP, Siberian Traps, Karoo LIP, etc.). Even so, the significance of the water enrichment in the mantle source has not been convincingly demonstrated for the generation of LIPs. A comparative study focusing on another volcanic province should be conducted; that province possesses other three melting conditions, such as, abnormally high temperature, substantial decompression, the presence of fusible components, but no water enrichment in the mantle source. The southeastern Asian basalt province (SABP) provides such a special case.

The SABP is composed of Cenozoic basalts with an age ranging from 28.5 Ma to <0.1 Ma. They mainly occur in the Leiqiong area, including the Leizhou Peninsula and the northern Hainan Island, and the Indochina block (Fig. 1a), being distributing over an area of about 0.037 Mkm^2 (hundreds of meters in thickness). Basalts in this province share common petrological and geochemical characteristics and their genesis has been related to the Hainan mantle plume (e.g., Wang et al., 2012, 2013; Liu J.Q. et al., 2015; An et al., 2017; Hoang et al., 2018; Yan et al., 2018). A mushroom-like seismic low-velocity anomaly, extending downward to the lower mantle, has been detected and suggests the existence of the lower mantle-rooted Hainan plume beneath this area (e.g., Lebedev and Nolet, 2003; Montelli et al., 2004; Huang et al., 2015; Xia S. et al., 2016). This is consistent with the presence of the transition zone of this area which is thinner than that of the normal mantle (Wei and Chen, 2016) and the calculated mantle potential temperature

(T_p) which is significantly higher than that of the ambient mantle (Wang et al., 2012; An et al., 2017). In addition, the area lies at the triple junction of the Eurasian, Indo-Australian and Pacific (Philippine) plates and is surrounded by multiple subduction zones. Subducted-slab structures penetrating into the lower mantle have been outlined by variations of the P wave velocity beneath this area (Li et al., 2008). The compositions of SABP basalts suggest the presence of pyroxenites in their mantle source (Wang et al., 2012; Liu J.Q. et al., 2015; An et al., 2017; Hoang et al., 2018), which can be produced by the reaction of subducted materials (or melts from them) with the ambient mantle (e.g., Sobolev et al., 2007; Herzberg, 2011). In spite of the favorable conditions (high T_p, the presence of fusible source components, and a decompressional setting by heating and lifting due to the Hainan plume, and fusible source components), the SABP is too small (0.037 Mkm^2 with a thickness of hundreds of meters; Hoang et al., 1996; Ho et al., 2000) to be a normal LIP (>0.1 Mkm^3; Ernst et al., 2005; Bryan and Ernst, 2008) (Fig. 1a). Given the four factors resulting in high melt production rates, it can be envisioned that the mantle source of the SABP was potentially poor in water, inhibiting the source rocks from melting in a large scale to produce voluminous melts for generation of a LIP. The water contents in the reconstructed primary basaltic melts in the SABP have been estimated (0.49–2.0 wt.%) by Wang et al. (2012) and An et al. (2017) on the basis of the Ce content and the assumed H_2O/Ce ratio of ~200, i.e., equal to an average ratio in oceanic basalts. However, this ratio displays a considerable variation in oceanic basalts (e.g., Michael, 1995; Dixon et al., 2002).

In this paper, we measured the water contents of early-crystallized clinopyroxene (Cpx) phenocrysts of Cenozoic basalts from the northern Hainan Island, a part of the SABP (Fig. 1), through which we retrieved the water content in the corresponding mantle source based on the approach that was used earlier by Xia et al. (2013) for Mesozoic primitive basalts of the North China Craton. The T_p value for the SABP is estimated to be similar to that of many LIPs and the contribution of fusible components (pyroxenites) in the mantle source of the SABP is re-verified. As the SABP is too small compared with a normal LIP, the particularity of the SABP highlights the significance of water enrichment in the generation of LIPs. The estimated low water content in the mantle source of Hainan basalts should imply that recycled materials should have significantly lost their water before their incorporation into the Hainan plume.

2. Samples

The Cenozoic Hainan basalts of the northern Hainan basalts are located in the center of the SABP (Fig. 1a). Furthermore, geophysical measurements have localized the Hainan plume beneath the northern part of the Hainan Island. Thus, the Hainan basalts provide appropriate samples to track the effects of the Hainan plume on the formation and evolution of the whole SABP.

Basaltic samples of this study were collected from three Cenozoic volcanoes located in the Leihuling mountain area and at the Chitucun village and the Yongxing town (Fig. 1b). The Chitucun basalts (CTC) erupted at about 0.46 Ma and the ages of the Leihuling (LHL) and Yongxing (YX) basalts are no more than 0.1 Ma (Ho et al., 2000; Wang et al., 2012). Most of the samples are fresh, displaying no observable alteration, which is also supported by the low values of loss on ignition (Table S1). All three suites of samples display a porphyritic texture with phenocrysts of olivine, clinopyroxene and Fe–Ti oxide (Fig. S1). Chemically, the CTC samples are olivine tholeiites and the Leihuling and Yongxing samples alkaline basalts (Fig. S2).

3. Analytical methods

The analytical methods are described in detail in the supplementary text. Major and trace element compositions of bulk-rock samples were analyzed using X-Ray fluorescence spectrometry and inductively coupled plasma mass spectrometry at ALS Chemex (Guangzhou, China) Co., Ltd. Mineral compositions were determined at the School of Earth Sciences, Zhejiang University, China. The water contents of Cpx phenocrysts were measured by Fourier transform infrared spectroscopy (FTIR) using unpolarized radiation. Major element compositions of olivine and Cpx phenocrysts were analyzed by a Shimadzu electron probe microanalyzer (EPMA 1720). The obtained major element compositions of Cpx phenocrysts were used to calculate the partition coefficient of water between Cpx and melt (O'Leary et al., 2010), which in turn were utilized in the estimation of the water content of the corresponding parental melts (Xia et al., 2013).

4. Results

4.1. Compositions of bulk rocks and phenocrysts

Major element compositions of bulk-rock samples are shown in Table S1. Tholeiites from Chitucun have MgO contents from 7.48 to 8.74 wt.%, being systematically lower than those in the LHL and YX alkali basalts (9.42–9.89 wt.%). This systematical chemical difference between tholeiites and alkali basalts is also reflected in the CaO, K_2O, TiO_2 and P_2O_5 contents (Table S1), being probably a reflection of different degrees of melting during their generation from the same mantle source.

Trace element compositions of bulk-rock samples are listed in Table S2. All the samples have OIB-like trace element distribution patterns, which are characterized by an enrichment of LREE and LILE, the presence of negative Pb anomalies, and the absence of negative Nb–Ta anomalies (Figs. S3a, b). The LHL and YX alkali basalts show higher REE contents and stronger LREE/HREE fractionation than tholeiites (Fig. S3a), indicating lower degrees of partial melting in the generation of the alkali basalts.

Compositions of olivine phenocrysts in the Hainan basalts are shown in Table S3. The CaO contents in olivine phenocrysts range from 0.19 to 0.34 wt.%, being higher than those in olivines from mantle peridotites (<0.1 wt.%; Thompson and Gibson, 2000). The NiO contents and Fe/Mn ratios in olivine phenocrysts vary from 0.19 to 0.37 wt.% and from 66 to 107, respectively, both being significantly higher than those in global MORBs at a given Mg# value (Figs. 2a, b). Moreover, the NiO contents and Fe/Mn ratios of olivine phenocrysts in the SABP basalts are similar to those in Hawaiian basalts and Dali picrites from the Emeishan LIP and slightly lower at a given Mg# value than those in basalts from the Siberian Traps and Karoo LIP (Figs. 2a, b).

4.2. Water contents in Cpx phenocrysts and the equilibrated melts

The infrared spectra of Cpx phenocrysts in the Hainan basalts display three groups of structural OH absorption bands, located at ~3640 cm^{-1}, ~3520 cm^{-1} and ~3460 cm^{-1} (Fig. S34a), which are comparable to those reported in the literature (e.g., Xia et al., 2013; Liu J. et al., 2015). Only considering the results obtained for Cpx phenocrysts with Mg# (= molar 100×Mg/(Mg+Fe)) higher than 75, the measured water contents in Cpx phenocrysts from the Hainan basalts range from 12 to 179 ppm, with an average of 61 ± 32 ppm (Table S4). The uncertainty of single analyses by FTIR has been estimated to be less than 30% (Xia et al., 2013; Liu J. et al., 2015). Combining the obtained Cpx water contents with the Cpx-melt partition coefficients of water calculated from the chemical composition of Cpx (equation (10) in O'Leary et al., 2010), we

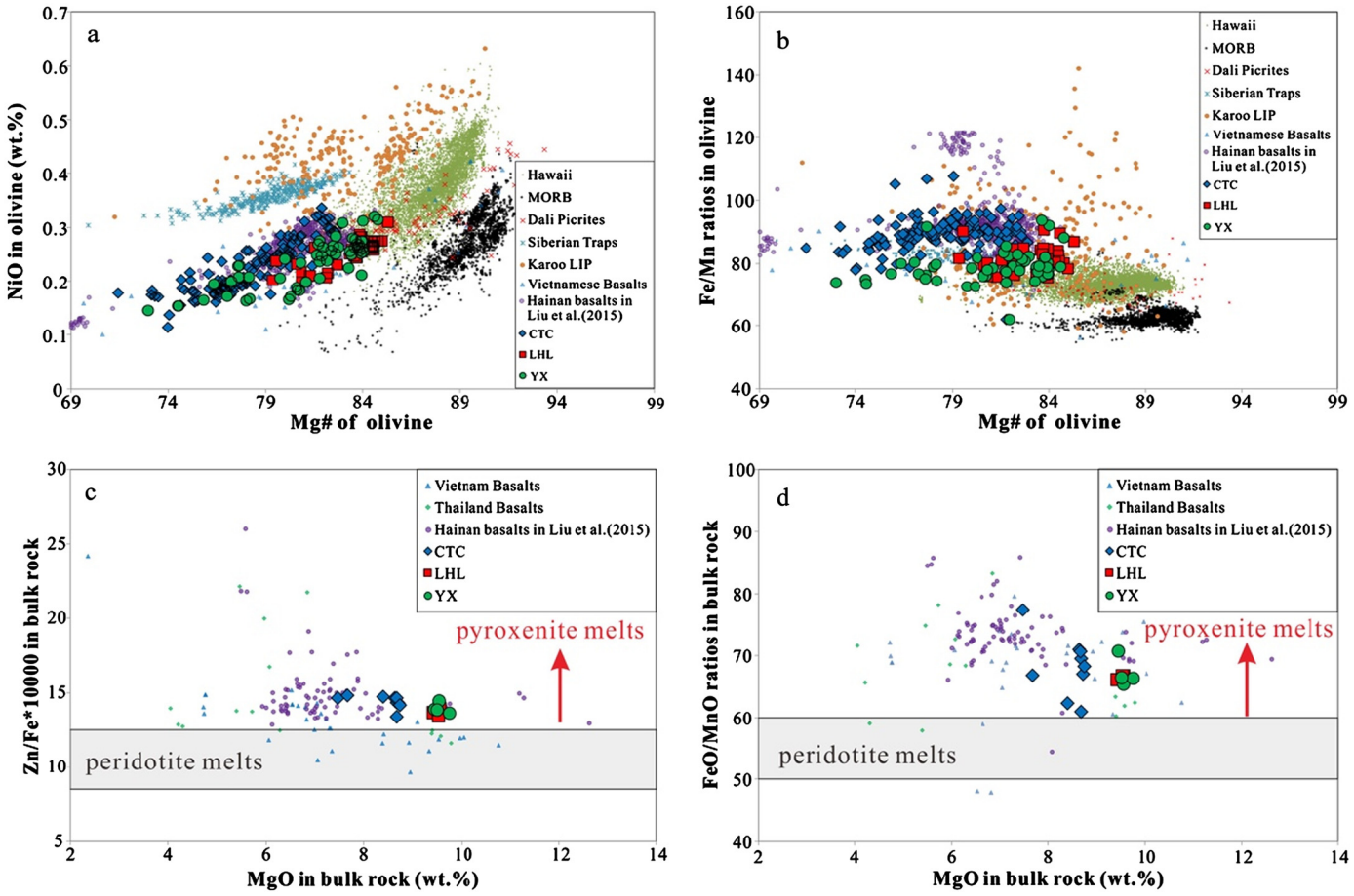

Fig. 2. Compositions of olivine phenocrysts and bulk rock samples suggesting contribution of pyroxenites in the mantle source of the Hainan basalts. (a) NiO contents in olivine phenocrysts plotted versus Fo (%). (b) Fe/Mn ratios in olivine phenocrysts plotted versus Fo (%). The data of MORBs, Hawaiian and Siberian basalts are from Sobolev et al. (2007), Karoo LIP basalts from Heinonen et al. (2013) and Dali picrites from Liu et al. (2017). (c) 1000∗Zn/Fe plotted against bulk-rock MgO contents. The ranges of 1000∗Zn/Fe values for peridotite and pyroxenite melts are from Le Roux et al. (2010). (d) FeO/MnO plotted against bulk-rock MgO contents. The FeO/MnO range of peridotite melts is from Herzberg (2011). In the four graphs, the data of Vietnamese basalts are from An et al. (2017) and Hoang et al. (2018). In (c) and (d), the Thai basalt data are from Yan et al. (2018). Hainan basalt data from Liu J.Q. et al. (2015) are also shown for comparison (points named as 'Hainan Basalts' in Liu J.Q. et al., 2015).

were able to determine water contents in the melts in equilibrium with Cpx, yielding a range from 0.28 to 1.24 wt.% and an average of 0.54 ± 0.29 wt.% (Table S5). The uncertainty in the calculation of the melt water contents is less than 40% (Xia et al., 2013; Liu J. et al., 2015). On the basis of the water contents of melts coupled with partial melting models (calculation details shown in the supplementary text), we also estimated the water content in the mantle source of the Hainan basalts. The obtained H_2O contents range from 84 to 360 ppm, with an average of 207 ppm (Table S5).

4.3. T_p estimation for the Hainan basalts

The initial crystallization temperatures of olivine (T_{ol}) in the primary melts of the Hainan basalts were estimated using different thermometers (Albarède, 1992; Putirka, 2008; Herzberg and Asimow, 2015). The compositions of the primary melts were reconstructed by incremental addition of olivine in equilibrium with the instantaneous melt compositions until the calculated magma was in equilibrium with olivine with Mg# = 90.7, which is the highest Mg# value of olivine phenocrysts reported from Hainan basalts (for calculation details, see the supplementary text). The temperatures estimated by the different thermometers display a similar range (Fig. S6) and are averaged for individual samples. The T_{ol} values range from 1468 to 1505 °C, having an average of 1481 ± 10 °C (Table S6), which are in agreement with previous estimates from basalts in the SABP (Fig. S6; Wang et al., 2012; An et al., 2017). Mantle potential temperatures were also calculated using the MgO (Herzberg and Gazel, 2009) and FeO (Kelley et al., 2006) contents in the primary melts. The calculated values from these two approaches show comparable ranges. We take the average value of 1521 ± 24 °C as the likely T_p value beneath the northern Hainan Island, which falls in the previously reported T_p range (Wang et al., 2012).

5. Discussion

5.1. Preservation of initial water contents in Cpx phenocrysts

To monitor the H diffusion potentially occurring after Cpx crystallization, FTIR profile analyses were conducted on a subset of Cpx phenocrysts. No differences in the band positions, band widths or peak heights can be observed in the obtained core-to-rim spectra (Fig. S5). Supposing that degassing had caused appreciable water loss from the parental magmas of the Hainan basalts, the Cpx phenocrysts should contain invariably low amounts of water. This is not the case as the water contents in different phenocrysts from a single sample and those in phenocrysts from different samples display a large variation (Table S4; Fig. S4b). Moreover, water loss by degassing after Cpx crystallization could trigger diffusive H loss from phenocrysts to coexisting melts and the larger grains should keep higher water contents than the smaller ones. The grain sizes of Cpx phenocrysts have been estimated under the microscope

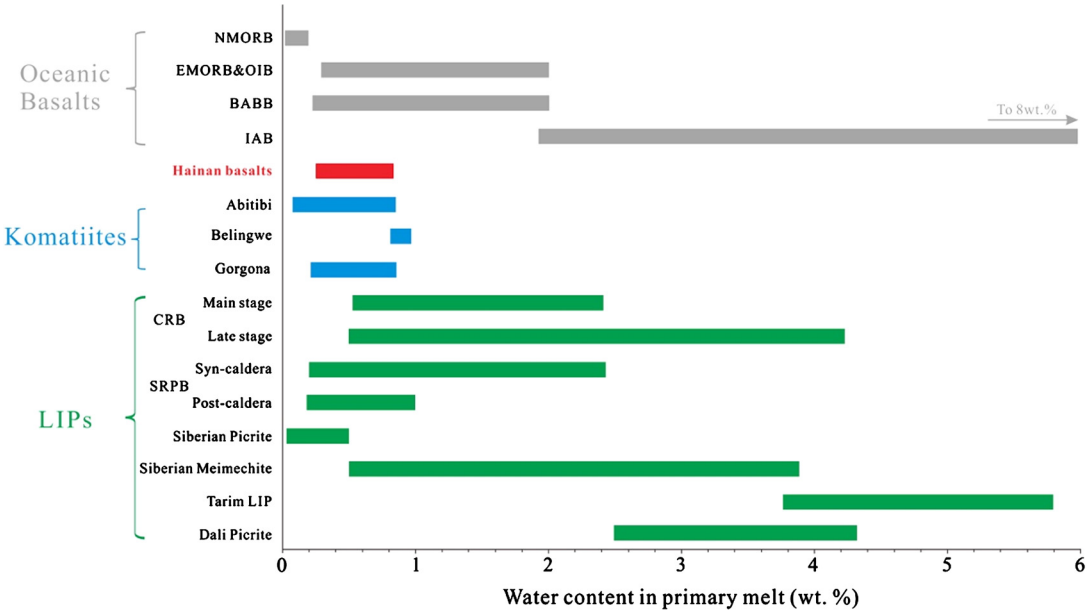

Fig. 3. Comparison of water contents in the primary melts of Hainan basalts with those in other primary melts from different geological settings. The water contents of the Siberian meimechites are from Ivanov et al. (2018) and those of other melts from Liu et al. (2017) and references therein. The Azorean basalts contain slightly more water (0.3–2.0 wt.%; Dixon et al., 2002; Métrich et al., 2014) than other OIBs and are included in 'EMORB & OIB' for comparison. The integral water content range for OIBs is much larger than that given by Dixon et al. (0.3–1.0 wt.%; 2004) when taking Azorean basalts into consideration. NMORB, normal mid-ocean ridge basalt; EMORB, enriched mid-ocean ridge basalt; OIB, oceanic island basalt; BABB, back-arc basin basalt; IAB, island arc basalt; CRB, Columbia River basalt; SRPB, Snake River Plain basalt.

or by means of BSE images. As demonstrated by two samples in Fig. S4c, no positive relationship can be observed between the grain size and water content. Therefore, water contents in Cpx phenocrysts of the Hainan basalts were not affected by degassing or mineral-melt diffusive water exchange after mineral crystallization and hence, the phenocrysts should have retained their initial compositions.

5.2. Water contents in the primary melts and mantle source of the Hainan basalts

The water content of Cpx measured by FTIR has an uncertainty of <30% for single analysis (Xia et al., 2013; Liu J. et al., 2015). Coupling this with the partitioning coefficient of water between Cpx and the basaltic melt calculated from the Cpx chemical composition (O'Leary et al., 2010), the water content of the melt in equilibrium with Cpx phenocryst can be calculated with an uncertainty <40% (Xia et al., 2013; Liu J. et al., 2015). In principle, the water content of a primary melt (referring to a primary melt formed in the mantle with minimal compositional modification after segregation with the source) should be recovered by the Cpx phenocrysts equilibrated with the earliest crystallized olivine phenocrysts, as indicated by the highest Mg# values. Experimental investigations have shown that, at the crystallization temperatures of olivine phenocrysts in the Hainan basalts (Table S6), the equilibrated Cpx and olivine phenocrysts should have similar Mg# (Loucks, 1996). However, most of the Cpx phenocrysts in the Hainan basalts have Mg# values lower than the highest Mg# values of the coexisting olivine phenocrysts (Tables S3 and S4), suggesting later crystallization. The simulated calculation demonstrated that, with fractional crystallization by different mineral assemblages from a basaltic melt, a decrease in Cpx Mg# by 15 units would be accompanied by less than 40% elevation in the water content of the melt (Liu J. et al., 2015). In addition, a compiled dataset of island arc basalts revealed that, with a decrease in the Mg# values of olivine phenocrysts by 15 units caused by fractional crystallization, the measured water contents in the primary melt inclusions hosted by olivines increase generally less than 30% (Plank et al., 2013). Therefore, the Cpx phenocrysts with Mg# values of <15 units lower than the highest Mg# values of the coexisting olivine phenocrysts can be used to recover the water content of the primary basaltic melt if the uncertainty of 40% is admitted. In the Hainan basalts, the highest Mg# of the olivine phenocrysts are ~85–90 for different basaltic volcanoes in the Hainan Island (Table S3; Wang et al., 2012; Liu J.Q. et al., 2015); therefore, only Cpx phenocrysts with Mg# of >75 were taken into consideration in the estimation of the water content in the primary melts. For every sample, multiple Cpx phenocrysts with Mg# of >75 were found and analyzed, and the average of the melt water contents calculated by these phenocrysts was used to represent the primary melt of that sample, with the uncertainty being expected to be less than 40% by using a single Cpx phenocryst. As a result, the water contents in the primary melts of the Hainan basalts can be estimated to range from 0.28 to 1.24 wt.%, with an average of 0.54 ± 0.29 wt.% (Table S5; Fig. 3).

Furthermore, we note that the calculated melt water contents for the CTC basalts (9 samples) display a prominent positive correlation with the concentrations of incompatible trace elements (e.g., Nb, La, Ce) in bulk rocks (Figs. 4a–c), similarly to the results obtained by Dixon et al. (2002) for undegassed ocean island basalts (OIBs) and mid-ocean-ridge basalts (MORBs). Progressive melting of the mantle can produce variable primary melts, in which water contents and incompatible element concentrations are positively correlated. These correlations suggest that the calculated water contents can represent the primary melt water contents and the use of Cpx phenocrysts to evaluate the water contents in primary melts is justified. For the LHL and YX samples, the correlations between the melt water contents and trace element concentrations are not conspicuous, except for Nb (Fig. 4d), which is likely due to the small number of studied samples (3 and 4 samples, respectively). Nonetheless, the LHL and YX samples are alkaline basalts and carry mantle peridotite xenoliths, indicating a faster ascent rate (O'Reilly and Griffin, 2010) than that of the CTC tholeiitic basalts. Therefore, we are confident that the calculated water contents of the LHL and YX melts are representative for their primary melts.

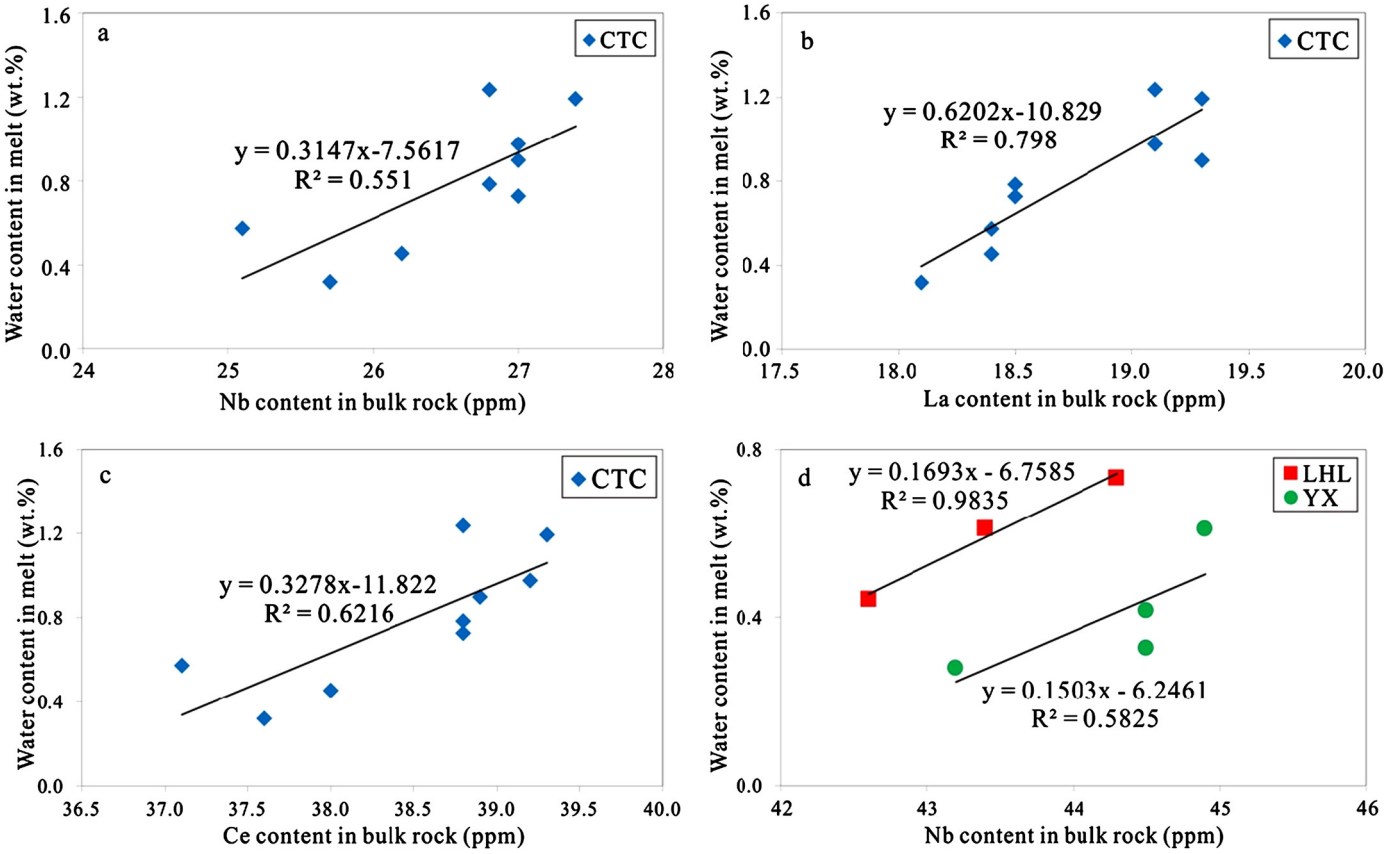

Fig. 4. Calculated melt water contents plotted against trace element concentrations in bulk rock samples of Hainan basalts. For each sample, the value is an average of melt water contents calculated using all Cpx phenocrysts with Mg# >75.

The calculated water contents for the primary magmas of the Hainan basalts fall in the range of the water contents of OIB magmas (0.3–2.0 wt.%; Dixon et al., 2004; Métrich et al., 2014) and are significantly lower than those in primary magmas of Phanerozoic LIPs (Fig. 3). Additionally, the water content in the mantle source of the Hainan basalts is significantly lower than those in the mantle sources of many LIPs (Fig. 5).

5.3. The factor inhibiting the SABP from forming a LIP

5.3.1. Hainan plume-induced high mantle potential temperature

We have calculated the mantle potential temperature of 1521 ± 24 °C beneath the northern Hainan Island. Similar values of T_p have also been reported for basalts from Vietnam (An et al., 2017). The high T_p beneath the SABP is similar to that beneath many LIPs and considerably higher than that of the MORB source (1350 ± 50 °C; Fig. 5) (Herzberg and Gazel, 2009; Liu et al., 2017). It suggests that the generation of the Hainan basalts are related to heating by the Hainan plume. The existence of the Hainan plume has been repeatedly demonstrated by the geophysical observations indicating the presence of a low seismic velocity anomaly down to the lower mantle (e.g., Montelli et al., 2004; Huang et al., 2015; Xia S. et al., 2016). Based on the seismic images, Xia S. et al. (2016) proposed that the Hainan plume spread laterally, generating a large head at depths of 350–500 km. Basalts in the SABP are distributed in a large area from the Leizhou Peninsula to Thailand, indicating that the Hainan plume head had spread across thousands of kilometers, being similar in extent to the estimated diameters of the plume heads responsible to the generation of many Phanerozoic LIPs (e.g., Emeishan LIP, Siberian Traps, etc.).

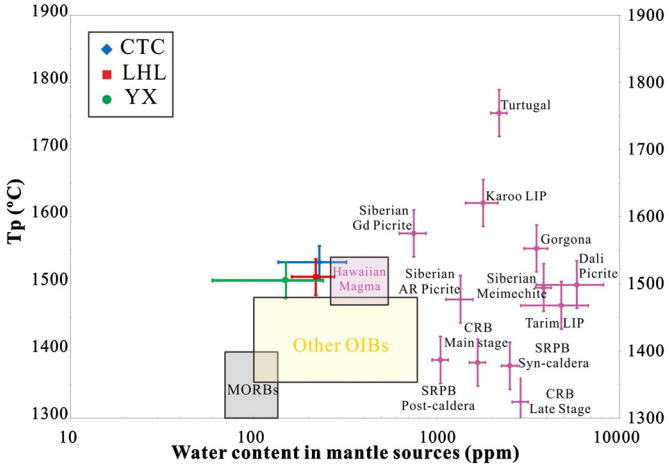

Fig. 5. Comparison of the water contents and T_p in the mantle sources of Hainan basalts, MORBs, OIBs and LIPs. The ranges of source water contents for MORBs, OIBs and the Hawaiian magma are from Bizimis and Peslier (2015). T_p for other OIBs and the Hawaiian magma are from Bizimis and Peslier (2015), after correction of the water effect. T_p for MORBs is the value necessary for the production of MORB with MgO content of 10–13% (Herzberg and Gazel, 2009). Water contents in the sources of LIPs are according to the compilation and calculation in Liu et al. (2017). T_p of LIPs are re-calculated in Liu et al. (2017) by the method of Herzberg and Gazel (2009). Gorgona and Tortugal represent komatiites and picrites from the Gorgona Island and Tortugal represent in the Caribbean LIP, respectively. Siberian AR and Gd picrites are the Ayan River picrite and Gudchikhinsky picrite from the Siberian Traps, respectively.

5.3.2. Pyroxenite-bearing mantle source for the SABP

Reactions of melts from subducted materials with peridotite (the dominant mantle constituent lithology; Sobolev et al., 2007)

or reactions between subducted materials and peridotite in the solid state (Herzberg, 2011) can produce pyroxenites, which are more fusible than peridotites. Different parameters have been proposed to trace the contribution of pyroxenites in the mantle source of basalts (Sobolev et al., 2007; Le Roux et al., 2010; Herzberg, 2011). The high NiO content and Fe/Mn ratio in olivine phenocrysts indicate involvement of pyroxenite in the generation of the Hainan basalts (Figs. 2a, b). This inference is supported by the systematically high FeO/MnO (Herzberg, 2011) and 1000∗Zn/Fe ratios (Le Roux et al., 2010) in bulk-rock compositions of the Hainan basalts (Table S1; Figs. 2c, d). The contribution of pyroxenite in the Hainan plume has also been proposed by previous studies (Figs. 2a–d; Wang et al., 2012; Liu J.Q. et al., 2015; An et al., 2017; Hoang et al., 2018).

5.3.3. Significance of the low water content in the Hainan plume mantle

In this study, abnormally high T_p induced by the Hainan plume and incorporation of pyroxenite in the mantle source were verified for the SABP, as represented by the Cenozoic basalts from the northern Hainan Island. These two factors are also present in many Phanerozoic LIPs (Liu et al., 2017). However, in contrast to many other LIPs with a >0.1 Mkm^3 volume of magmas emplaced in pulses of less than 5 Ma, the SABP has a clearly lower melt production rate (<0.04 Mkm^3 in a time period from 28.5 to <0.1 Ma).

In the Hainan basalts, the Nb/U and Ce/Pb ratios range from 27.9 to 46.8 and from 13 to 21.9, respectively. Both range are similar to those in MORBs and OIBs and much higher than those in the continental crust (Hofmann et al., 1986), suggesting an insignificant degree of crustal contamination (Fig. S7). Recent geochemical studies have demonstrated that the Hainan basalts experienced little assimilation of sub-continental lithospheric mantle during their ascent to the surface (Fig. S7; Wang et al., 2013; Liu J.Q. et al., 2015; Zou and Fan, 2010). All these aspects together point to the conclusion that the Hainan basalts are partial melts of lower mantle-derived components of the Hainan plume. Consequently, the relatively low water contents in the source of the Hainan basalts mean that the Hainan plume was dry relative to the plumes associated with many other Phanerozoic LIPs.

It has been shown experimentally that the presence of water in mantle minerals, even in tiny amounts, can drastically influence the viscosity (η) of the mantle; the more water the mantle contains, the more η is decreased (Hirth and Kohlstedt, 1996; Dixon et al., 2004). The relatively lower water content in the Hainan plume can induce a higher viscosity compared to other plumes that generated LIPs. Using the calculation model of Dixon et al. (2004) and Peslier et al. (2010), it can be shown that the low water content in the Hainan plume (80 to 360 ppm, with an average of 207 ppm) results in a mantle η value that is >50 times higher than η in the source of the Emeishan LIP (up to 6000 ppm; Liu et al., 2017), considering the water content as the only variable (see the supplementary text for details).

According to the foregoing discussion, the Hainan basalts are regarded as direct partial melts of plume-delivered materials. The high melt production rate necessary to a LIP, facilitated by elevated T_p and significant decompression, requires prompt continuous mass and energy feeding to the mantle source. For basalts stemming from a deep mantle-rooted plume, the mass supply flux depends on the plume upwelling velocity (W), which is usually considered to be controlled by the thermal buoyancy of the plumes. Given that the seismic low-velocity anomaly induced by the Hainan plume has a mushroom-like geometry (Xia S. et al., 2016), the Hainan plume can be regarded as a diapiric plume (Olson and Singer, 1985). Experimental simulation has revealed that, for a diapiric plume, W is inversely proportional to η of the mantle plume ($W \propto 1/\eta$; Olson and Singer, 1985). Therefore, compared with hydrous mantle plumes underlying many Phanerozoic LIPs, the relatively low water content in the Hainan plume made it ascend with a lower velocity, which is consistent with the relatively high excess of ^{230}Th (as high as 32%) detected in two Holocene Hainan volcanoes (one of them also studied here; Zou and Fan, 2010). The slow upwelling rate of the Hainan plume led to a deficient mass supply flux for the SABP, diminishing its melt production rate.

Additionally, the upwelling of the mantle plume depends on the buoyancy, which is intimately related to the viscosity contrast between the plume and its ambient mantle. A low water content induces a high viscosity for the starting plume, which means that the viscosity contrast of the dry plume with its ambient mantle is also relatively lower. The viscosity of the mantle generally increases with depths (Hansen et al., 1993). During upwelling of a dry mantle plume, the viscosity of the ambient mantle decreases and the viscosity contrast gradually diminishes. We suggest that the plume will stall at a depth where the viscosity contrast is insufficient to drive the upwelling. In the Hainan plume case, this phenomenon is reflected in the observation of Xia S. et al. (2016), according to which a large seismic low-velocity anomaly exists at depths of 350–500 km beneath the Hainan Island, perhaps corresponding to the cease of upwelling, the ponding of plume materials and the formation of the plume head (Fig. 6). Persistent heat supply from the plume tail made the head unstable and drove multiple occasional and small diapirs to rise upwards from the top of the head (Fig. 6). During their ascent, materials in the diapirs, including pyroxenites originally related to subducted materials, underwent decompression-induced melting, resulting in small-scale magmatism, such as that represented by the Hainan basalts. Due to the long-lasting, slow but intermittent upwelling of the Hainan plume, the basalts of the SABP were emplaced over a long period of time, from 28.5 Ma to <0.1 Ma, but did not produce voluminous eruptions.

Furthermore, model calculations of hydrous melting of oceanic mantle indicate that addition of water can significantly enhance the total melt production by deepening the onset of melting (Asimow and Langmuir, 2003). The low water content potentially causes a lower melt production of the diapirs stemming from the Hainan plume compared to LIP-generating plumes, given the same mass of plume-delivered material.

In terms of all the melting conditions caused by mantle plumes, the prominent difference of the Hainan plume compared with LIP-related plumes lies in the water contents. Based on the above discussion, we suggest that the low water content in the Hainan plume played a key role in the cessation of the LIP formation in southeastern Asia, despite the presence of other favorable conditions, such as high T_p, decompression, and the contribution of fusible components in the mantle source.

5.3.4. A model for the generation of the SABP

A series of geophysical studies revealed that the Hainan plume should be associated with the deep subduction of the Pacific and Philippine Sea slabs in the east and that of the Indian slab in the west down to the lower mantle (Zhao et al., 2011 and references therein). And the subducted-slab structures penetrating into the lower mantle have been outlined by variations of the P wave velocity beneath this area (Li et al., 2008). Wang et al. (2013) combined seismic, geochemical and geological observations, and proposed that the subsidence of the Indian and Pacific slabs to the core-mantle boundary stimulated and contributed to the thermochemical upwelling forming the Hainan plume. Moreover, Zhang and Li (2018) conducted 3D geodynamic modeling to reveal the feasibility of the Hainan plume driven by the nearby subducting slabs surrounding the South China Sea region. Several studies have presented geochemical and isotopic evidence supporting that the Hainan basalts might have been derived from partial melting of

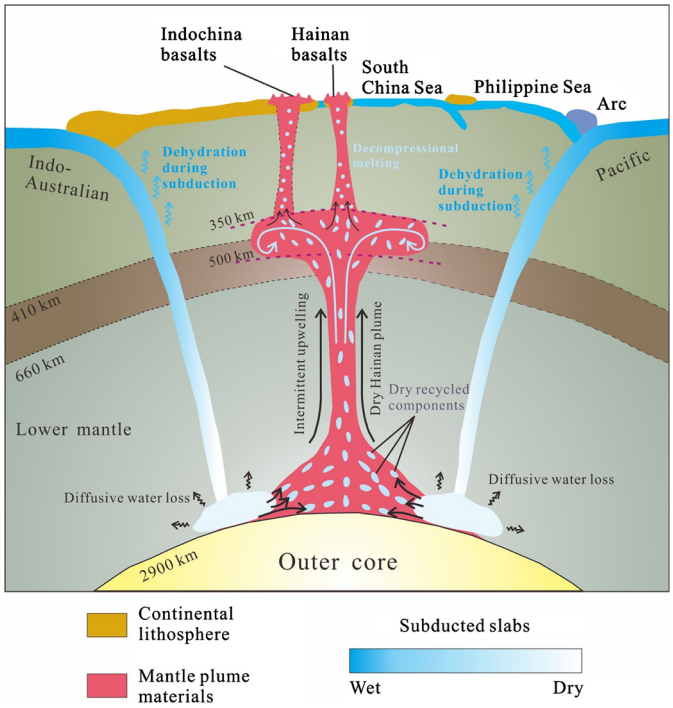

Fig. 6. Cartoon illustrating the generation of the dry Hainan plume and the formation of the SABP (modified from Wang et al., 2013). Several lines of geophysical and geochemical evidence support the view that recycled components from the Indo-Australian subducted slab or Pacific slab have percolated into the Hainan plume source (e.g., Zhao et al., 2011; Wang et al., 2013; Zhang and Li, 2018), as illustrated by thin and filled arrows. Both mechanisms, dehydration during subduction and diffusive water loss in the inner mantle, possibly account for the dehydration of subducted slabs (Dixon et al., 2002; Workman et al., 2006). The high viscosity induced by the low water content resulted in the ponding of plume-delivered material at depths of 350–500 km, forming a plume head. This is consistent with the large seismic low-velocity anomaly observed at these depths by Xia S. et al. (2016). Persistent heat supply from the plume tail made the head unstable and drove multiple occasional small diapirs to rise upwards from the top of the head. During its ascent, material delivered by the diapirs, including pyroxenites originally associated with subducted material, underwent decompression-induced melting, resulting in small-scale magmatism, such as represented by the Hainan basalts. Due to the long-lasting, slow but intermittent upwelling of the Hainan plume, the basalts of the SABP were emplaced over a long period of time from 28.5 Ma to <0.1 Ma but never in large volumes.

plume-delivered lower mantle materials enriched with the recycled components (e.g., Zou and Fan, 2010; Wang et al., 2012, 2013; Liu J.Q. et al., 2015). Thus, we can conclude that the subducted materials have assembled at the core-mantle boundary and contributed to the Hainan plume. The calculated water contents for the primary magmas of the Hainan basalts (0.28–1.24 wt.%) fall in the range of the water contents of OIB magmas (0.3–2.0 wt.%; Dixon et al., 2004; Métrich et al., 2014) and are significantly lower than those of primary magmas in Phanerozoic LIPs (Fig. 3). It means that the Hainan plume was dry relative to the plumes associated with many other Phanerozoic LIPs.

The slight variation of the H_2O/Ce content ratio in oceanic basalts on a local scale implies similar incompatibility of these two elements during partial melting of the mantle (Micheal, 1995). And the variable H_2O/Ce ratios in basaltic melts can reflect a distinct feature of their mantle sources and even delineate the source evolution. The sources of MORBs have been estimated to have H_2O/Ce ratios of 150–210 (Micheal, 1995; Dixon et al., 2002). For many Phanerozoic LIPs, H_2O/Ce ratios in their sources range from ~160–400 to >2000 (Liu et al., 2017). In contrast, the H_2O/Ce ratio in the source of Hainan basalts is estimated to range from 50 to 319, being mostly lower than 150 (Table S5), indicating the recycled component in the mantle source of Hainan basalts is relatively dry. Dixon et al. (2002) have proposed that the recycled oceanic crust in the mantle source of EM basalts (H_2O/Ce < 100) underwent intense dehydration (>92%) during subduction. In addition, Workman et al. (2006) suggested that the diffusive loss of water to the ambient mantle during the aging/storage of oceanic slabs within the mantle also contributed to the formation of the dry EM endmember component. Oceanic crust components revealed in the Hainan basalts subducted from the surface to the lower mantle and were likely to experience the fore-mentioned dehydration processes. Thus, the low water content in the mantle source of the Hainan plume can be attributed to the incorporation of subducted slabs that have experienced significant dehydration (Fig. 6).

In summary, as shown in Fig. 6, we suggest that the subduction of the Indian and Pacific slabs to the core-mantle boundary stimulated and contributed to the thermochemical upwelling to form the plume. The recycled components have undergone significant dehydration and the contribution of these recycled components induced the Hainan plume to be dry. As discussed above, we propose that the low water content lowers the viscosity, resulting in the Hainan plume upwelling slowly and stalling at depths of 350–500 km, where plume materials pond to form the plume head. The persistent heat supply from the plume tail makes the head unstable and drives the formation of occasional and small diapirs. During ascent of these diapirs, decompression-induced melting occurs and produces the small-scale magmatism like the Hainan basalts. Furthermore, the low water content can also reduce the melt production of the materials in the small ascending diapirs stemming from the Hainan plume. The long-lasting, slow but intermittent upwelling of the Hainan plume and low speed of melt production lead to the low volume and long formation period of the SABP compared with many Phanerozoic LIPs. Thus, like other plumes generating LIPs, the Hainan plume have the characteristics of high T_p and the contribution of fusible components in the mantle source, but the low water content resulted in the Hainan plume not generating a normal LIP.

5.4. Implications for the headless plumes

Experimental simulations revealed that a starting plume is composed of a large bulbous head followed by a narrow conduit (e.g., Olson and Singer, 1985). It has been proposed that heads of mantle starting plumes melt and generate LIPs, while the following conduits continue melting to form the hotspot tracks (Richards et al., 1989; Campbell and Griffiths, 1990; Campbell, 2007). However, recent studies found that some volcanic chains cannot be traced back to link with LIPs (e.g., Pitcairn, Azores, Samoa, etc.; Courtillot et al., 2003) and they seem to be generated by plume tails without heads. The genesis of these headless plumes is still hotly debated. Numerically modeling indicates that the headless plume originating from the deep mantle can be stirred by chemical heterogeneities and the surface expression may be age-progressive volcanic chains (Farnetani and Samuel, 2005). In the model of Farnetani and Samuel (2005), the starting plume stalls at the 670 km discontinuity. The low-density components can break away from the parent plume, penetrate the transition zone and form a small plume. Then, the severe upper mantle shear tilts the conduits of the small plume. It is worth noting that the OIBs originally related to headless plumes contain similar low water contents with Hainan basalts (Fig. 3), which means these headless plumes should also be relatively dry. For the Hainan plume, our research suggests that the low water content can significantly influence the upwelling of the plume. Therefore, studies on water contents in the headless plumes may provide an alternative perspective to investigate the formation of the headless plumes.

6. Conclusion

Water contents of high-Mg# clinopyroxene phenocrysts from Cenozoic Hainan basalts, representatives of the products of the southeastern Asian basalt province (SABP), were measured with FTIR, yielding concentrations of 12–179 ppm. Based on these results, the water content in the mantle source of the SABP was estimated to range from 84 to 360 ppm, being significantly lower than those estimated for many Phanerozoic LIPs. The presence of fusible components in the source of the SABP is supported by the major element compositions of the basalts and their olivine phenocrysts. In combination with previously reported data, our results indicate that the mantle potential temperature for the SABP was ~170 °C higher than that for the MORB source mantle. Compared to many Phanerozoic LIPs, the significantly low water content in the mantle source of the SABP is likely the key factor that inhibited the SABP from forming a LIP in response to the upwelling Hainan plume. The low source water content of the Hainan basalts suggests that the Hainan plume entrained subducted slabs whose water had been extracted to a large extent before their transfer to the plume source. Accordingly, the SABP, as a counterexample, corroborates the view that water enrichment in the mantle source can play a significant role in facilitating the generation of LIPs. Enrichment of water in the plumes works in combination with other factors, such as an abnormally high temperature, substantial decompression, and the presence of fusible components, to generate LIPs.

Acknowledgements

This study was supported by the Strategic Priority Research Program (B) of Chinese Academy of Sciences (grant no. XDB18000000) and the National Natural Science Foundation of China (grant nos. 41702046 and 41630205). We thank the two reviewers, Jacqueline Eaby Dixon and Val Finlayson, for their constructive comments, and Tamsin Mather for her editorial handling.

Appendix A. Supplementary material

Supplementary material related to this article can be found online at https://doi.org/10.1016/j.epsl.2019.03.034.

References

Albarède, F., 1992. How deep do common basaltic magmas form and differentiate. J. Geophys. Res. 97, 10997–11009. https://doi.org/10.1029/91JB02927.

An, A.R., Choi, S.H., Yu, Y., Lee, D.C., 2017. Petrogenesis of Late Cenozoic basaltic rocks from southern Vietnam. Lithos 272, 192–204. https://doi.org/10.1016/j.lithos.2016.12.008.

Asimow, P.D., Langmuir, C.H., 2003. The importance of water to oceanic mantle melting regimes. Nature 421, 815–820. https://doi.org/10.1038/nature01429.

Bizimis, M., Peslier, A.H., 2015. Water in Hawaiian garnet pyroxenites: implications for water heterogeneity in the mantle. Chem. Geol. 397, 61–75. https://doi.org/10.1016/j.chemgeo.2015.01.008.

Bryan, S.E., Ernst, R.E., 2008. Revised definition of Large Igneous Provinces (LIPs). Earth-Sci. Rev. 86, 175–202. https://doi.org/10.1016/j.earscirev.2007.08.008.

Cabato, J.A., Stefano, C.J., Mukasa, S.B., 2015. Volatile concentrations in olivine-hosted melt inclusions from the Columbia River flood basalts and associated lavas of the Oregon Plateau: implications for magma genesis. Chem. Geol. 392, 59–73. https://doi.org/10.1016/j.chemgeo.2014.11.015.

Campbell, I.H., 2001. Identification of ancient mantle plumes. In: Ernst, R.E., Buchan, K.L. (Eds.), Mantle Plumes: Their Identification Through Time. In: Geol. Soc. Am., Spec. Pap., vol. 352, pp. 5–21.

Campbell, I.H., 2007. Testing the plume theory. Chem. Geol. 241, 153–176. https://doi.org/10.1016/j.chemgeo.2007.01.024.

Campbell, I.H., Griffiths, R.W., 1990. Implications of mantle plume structure for the evolution of flood basalts. Earth Planet. Sci. Lett. 99, 79–93. https://doi.org/10.1016/0012-821X(90)90072-6.

Courtillot, V., Davaille, A., Besse, J., Stock, J., 2003. Three distinct types of hotspots in the Earth's mantle. Earth Planet. Sci. Lett. 205, 295–308. https://doi.org/10.1016/S0012-821X(02)01048-8.

Dixon, J.E., Leist, L., Langmuir, C., Schilling, J.G., 2002. Recycled dehydrated lithosphere observed in plume-influenced mid-ocean-ridge basalt. Nature 420, 385–389. https://doi.org/10.1038/nature01215.

Dixon, J.E., Dixon, T.H., Bell, D.R., Malservisi, R., 2004. Lateral variation in upper mantle viscosity: role of water. Earth Planet. Sci. Lett. 222, 451–467. https://doi.org/10.1016/j.epsl.2004.03.022.

Ernst, R.E., Buchan, K.L., Campbell, I.H., 2005. Frontiers in large igneous province research. Lithos 79, 271–297. https://doi.org/10.1016/j.lithos.2004.09.004.

Farnetani, C.G., Samuel, H., 2005. Beyond the thermal plume paradigm. Geophys. Res. Lett. 32, 303–341. https://doi.org/10.1029/2005GL022360.

Hales, T.C., Abt, D.L., Humphreys, E.D., Roering, J.J., 2005. A lithospheric instability origin for Columbia River flood basalts and Wallowa Mountains uplift in northeast Oregon. Nature 438, 842–845. https://doi.org/10.1038/nature04313.

Hansen, U., Yuen, D.A., Kroening, S.E., Larsen, T.B., 1993. Dynamical consequences of depth-dependent thermal expansivity and viscosity on mantle circulations and thermal structure. Phys. Earth Planet. Inter. 77, 201–223. https://doi.org/10.1016/0031-9201(93)90099-U.

Heinonen, J.S., Luttinen, A.V., Riley, T.R., Michallik, R.M., 2013. Mixed pyroxenite–peridotite sources for mafic and ultramafic dikes from the Antarctic segment of the Karoo continental flood basalt province. Lithos 177, 366–380. https://doi.org/10.1016/j.lithos.2013.05.015.

Herzberg, C., 2011. Identification of source lithology in the Hawaiian and Canary islands: implications for origins. J. Petrol. 52, 113–146. https://doi.org/10.1093/petrology/egq075.

Herzberg, C., Asimow, P.D., 2015. PRIMELT3 MEGA.XLSM software for primary magma calculation: peridotite primary magma MgO contents from the liquidus to the solidus. Geochem. Geophys. Geosyst. 16, 563–578. https://doi.org/10.1002/2014GC005631.

Herzberg, C., Gazel, E., 2009. Petrological evidence for secular cooling in mantle plumes. Nature 458, 619–622. https://doi.org/10.1038/nature07857.

Hirth, G., Kohlstedt, D.L., 1996. Water in the oceanic upper mantle: implications for rheology, melt extraction and the evolution of the lithosphere. Earth Planet. Sci. Lett. 144, 93–108. https://doi.org/10.1016/0012-821X(96)00154-9.

Ho, K.S., Chen, J.C., Juang, W.S., 2000. Geochronology and geochemistry of late Cenozoic basalts from the Leiqiong area, southern China. J. Asian Earth Sci. 18, 307–324. https://doi.org/10.1016/S1367-9120(99)00059-0.

Hoang, N., Flower, M.F.J., Carlson, R.W., 1996. Major, trace element, and isotopic compositions of Vietnamese basalts: interaction of hydrous EM1-rich asthenosphere with thinned Eurasian lithosphere. Geochim. Cosmochim. Acta 60, 4329–4351. https://doi.org/10.1016/S0016-7037(96)00247-5.

Hoang, T.H.A., Choi, S.H., Yu, Y., Pham, T.H., Nguyen, K.H., Ryu, J.S., 2018. Geochemical constraints on the spatial distribution of recycled oceanic crust in the mantle source of late Cenozoic basalts, Vietnam. Lithos 296–299, 382–395. https://doi.org/10.1016/j.lithos.2017.11.020.

Hofmann, A.W., Jochum, K.P., Seifert, M., White, W.M., 1986. Nb and Pb in oceanic basalts: new constraints on mantle evolution. Earth Planet. Sci. Lett. 79, 33–45. https://doi.org/10.1016/0012-821X(86)90038-5.

Hole, M.J., 2015. The generation of continental flood basalts by decompression melting of internally heated mantle. Geology 43, 311–314. https://doi.org/10.1130/g36442.1.

Huang, Z., Zhao, D., Wang, L., 2015. P wave tomography and anisotropy beneath southeast Asia: insight into mantle dynamics. J. Geophys. Res. 120, 5154–5174. https://doi.org/10.1002/2015JB012098.

Ivanov, A.V., Mukasa, S.B., Kanmenetsky, V.S., Ackerson, M., Demonterova, E.I., Pokrovsky, B.G., Vladykin, N.V., Kolesnichenko, M.V., Litasov, K.D., Zedgenizov, D.A., 2018. Volatile concentrations in olivine-hosted melt inclusions from meimechite and melanephelinite lavas of the Siberian Traps Large Igneous Province: evidence for flux-related high-Ti, high-Mg magmatism. Chem. Geol. 483, 442–462. https://doi.org/10.1016/j.chemgeo.2018.03.011.

Jones, A.P., Price, G.D., Price, N.J., DeCarli, P.S., Clegg, R.A., 2002. Impact induced melting and the development of large igneous provinces. Earth Planet. Sci. Lett. 202, 551–561. https://doi.org/10.1016/S0012-821X(02)00824-5.

Kelley, K.A., Plank, T., Grove, T.L., Stolper, E.M., Newman, S., Hauri, E., 2006. Mantle melting as a function of water content beneath back-arc basins. J. Geophys. Res. 111, B09208. https://doi.org/10.1029/2005JB003732.

Le Roux, V., Lee, C.-T.A., Turner, S.J., 2010. Zn/Fe systematics in mafic and ultramafic systems: implications for detecting major element heterogeneities in the Earth's mantle. Geochim. Cosmochim. Acta 74, 2779–2796. https://doi.org/10.1016/j.gca.2010.02.004.

Lebedev, S., Nolet, G., 2003. Upper mantle beneath Southeast Asia from S velocity tomography. J. Geophys. Res. 108, 2048. https://doi.org/10.1029/2000JB000073.

Li, C., Hilst, R.D.V.D., Engdahl, E.R., Burdick, S., 2008. A new global model for P wave speed variations in Earth's mantle. Geochem. Geophys. Geosyst. 9, Q05018. https://doi.org/10.1029/2007GC001806.

Liu, J., Xia, Q.K., Deloule, E., Ingrin, J., Chen, H., Feng, M., 2015. Water content and oxygen isotopic composition of alkali basalts from the Taihang Mountains, China: recycled oceanic components in the mantle source. J. Petrol. 56, 1–22. https://doi.org/10.1093/petrology/egv013.

Liu, J., Xia, Q.K., Kuritani, T., Hanski, E., Yu, H.R., 2017. Mantle hydration and the role of water in the generation of large igneous provinces. Nat. Commun. 8, 1824. https://doi.org/10.1038/s41467-017-01940-3.

Liu, J.Q., Ren, Z.Y., Nichols, A.R.L., Song, M.S., Qian, S.P., Zhang, Y., Zhao, P.P., 2015. Petrogenesis of late Cenozoic basalts from North Hainan Island: constraints from melt inclusions and their host olivines. Geochim. Cosmochim. Acta 152, 89–121. https://doi.org/10.1016/j.gca.2014.12.023.

Loucks, R.R., 1996. A precise olivine-augite Mg–Fe-exchange geothermometer. Contrib. Mineral. Petrol. 125, 140–150. https://doi.org/10.1007/s004100050211.

Métrich, N., Zanon, V., Créon, L., Hildenbrand, A., Moreira, M., Marques, F.O., 2014. Is the 'Azores hotspot' a wetspot? Insights from the geochemistry of fluid and melt inclusions in olivine of Pico basalts. J. Petrol. 55, 377–393. https://dioi.org/10.1093/petrology/egt071.

Michael, P., 1995. Regionally distinctive sources of depleted MORB: evidence from trace elements and H_2O. Earth Planet. Sci. Lett. 131, 301–320. https://doi.org/10.1016/0012-821X(95)00023-6.

Montelli, R., Nolet, G., Dahlen, F.A., Masters, G., Engdahl, E.R., Hung, S.H., 2004. Finite-frequency tomography reveals a variety of plumes in the mantle. Science 303, 338–343. https://doi.org/10.1126/science.1092458.

O'Leary, J.A., Gaetani, G.A., Hauri, E.H., 2010. The effect of tetrahedral Al^{3+} on the partitioning of water between clinopyroxene and silicate melt. Earth Planet. Sci. Lett. 297, 111–120. https://doi.org/10.1016/j.epsl.2010.06.011.

Olson, P., Singer, H., 1985. Creeping plumes. J. Fluid Mech. 158, 511–531. https://doi.org/10.1017/S0022112085002749.

O'Reilly, S.Y., Griffin, W.L., 2010. Rates of magma ascent: constraints from mantle-derived xenoliths. In: Dosseto, A., Turner, A.P., Van Orman, J.A. (Eds.), Timescales of Magmatic Processes: From Core to Atmosphere. John Wiley & Sons, Ltd., Chichester, UK, pp. 116–124.

Peslier, A.H., Woodland, A.B., Bell, D.R., Lazarov, M., 2010. Olivine water contents in the continental lithosphere and the longevity of cratons. Nature 467, 78–81. https://doi.org/10.1038/nature09317.

Plank, T., Kelley, K.A., Zimmer, M.M., Hauri, E.H., Wallace, P.J., 2013. Why do mafic arc magmas contain ~4 wt% water on average? Earth Planet. Sci. Lett. 364, 168–179. https://doi.org/10.1016/j.epsl.2012.11.044.

Putirka, K.D., 2008. Thermometers and barometers for volcanic systems. Rev. Mineral. Geochem. 69, 61–120. https://doi.org/10.2138/rmg.2008.69.3.

Richards, M.A., Duncan, R.A., Courtillot, V.E., 1989. Flood basalts and hot-spot tracks: plume heads and tails. Science 246, 103–107. https://doi.org/10.1126/science.246.4926.103.

Sobolev, A.V., Hofmann, A.W., Kuzmin, D.V., Yaxley, G.M., Arndt, N.T., Chung, S.L., Danyushevsky, L.V., Elliott, T., Frey, F.A., Garcia, M.O., Gurenko, A.A., Kamenetsky, V.S., Kerr, A.C., Krivolutskaya, N.A., Matvienkov, V.V., Nikogosian, I.K., Rocholl, A., Sigurdsson, I.A., Sushchevskaya, N.M., Teklay, M., 2007. The amount of recycled crust in sources of mantle-derived melts. Science 316, 412–417. https://doi.org/10.1126/science.1138113.

Thompson, R.N., Gibson, S.A., 2000. Transient high temperatures in mantle plume heads inferred from magnesian olivines in Phanerozoic picrites. Nature 407, 502–506. https://doi.org/10.1038/35035058.

Wang, X.C., Li, Z.X., Li, X.H., Li, J., Liu, Y., Long, W.G., Zhou, J.B., Wang, F., 2012. Temperature, pressure, and composition of the mantle source region of late Cenozoic basalts in Hainan Island, SE Asia: a consequence of a young thermal mantle plume close to subduction zones? J. Petrol. 53, 177–233. https://doi.org/10.1093/petrology/egr061.

Wang, X.C., Li, Z.X., Li, X.H., Li, J., Xu, Y.G., Li, X.H., 2013. Identification of an ancient mantle reservoir and young recycled materials in the source region of a young mantle plume: implications for potential linkages between plume and plate tectonics. Earth Planet. Sci. Lett. 377–378, 248–259. https://doi.org/10.1016/j.epsl.2013.07.003.

Wei, S.S., Chen, Y.J., 2016. Seismic evidence of the Hainan mantle plume by receiver function analysis in southern China. Geophys. Res. Lett. 43, GL069513. https://doi.org/10.1002/2016GL069513.

Workman, R.K., Hauri, E., Hart, S.R., Wang, J., Blusztajn, J., 2006. Volatile and trace elements in basaltic glasses from Samoa: implications for water distribution in the mantle. Earth Planet. Sci. Lett. 241, 932–951. https://doi.org/10.1016/j.epsl.2005.10.028.

Xia, Q.K., Liu, J., Liu, S.C., Kovács, I., Feng, M., Dang, L., 2013. High water content in Mesozoic primitive basalts of the North China Craton and implications on the destruction of cratonic mantle lithosphere. Earth Planet. Sci. Lett. 361, 85–97. https://doi.org/10.1016/j.epsl.2012.11.024.

Xia, Q.K., Bi, Y., Tian, W., Wei, X., Chen, H.L., 2016. High water content in primitive continental flood basalts. Sci. Rep. 6, 25416. https://doi.org/10.1038/srep25416.

Xia, S., Zhao, D., Sun, J., Huang, H., 2016. Teleseismic imaging of the mantle beneath southernmost China: new insights into the Hainan plume. Gondwana Res. 36, 33–43. https://doi.org/10.1016/j.gr.2016.05.003.

Yan, Q., Shi, X., Metcalfe, I., Liu, S., Xu, T., Kornkanitnan, N., Sirichaiseth, T., Yuan, L., Zhang, Y., Zhang, H., 2018. Hainan mantle plume produced late Cenozoic basaltic rocks in Thailand, Southeast Asia. Sci. Rep. 8, 2640. https://doi.org/10.1038/s41598-018-20712-7.

Zhang, N., Li, Z.X., 2018. Formation of mantle "lone plumes" in the global downwelling zone – a multiscale modelling of subduction-controlled plume generation beneath the South China Sea. Tectonophysics 723, 1–13. https://doi.org/10.1016/j.tecto.2017.11.038.

Zhao, D., Yu, S., Ohtani, E., 2011. East Asia: seismotectonics, magmatism and mantle dynamics. J. Asian Earth Sci. 40, 6890–7090. https://doi.org/10.1016/j.jseaes.2010.11.013.

Zou, H., Fan, Q., 2010. U-Th isotopes in Hainan basalts: implications for subasthenospheric origin of EM2 mantle endmember and the dynamics of melting beneath Hainan Island. Lithos 116, 145–152. https://doi.org/10.1016/j.lithos.2010.01.010.